CEBAF PROPOSAL COVER SHEET

A. TITLE: A Measurement of Rare Radiative Decays of the ϕ Meson

B. CONTACT PERSON: Alex R. Dzierba

ADDRESS, PHONE AND ELECTRONIC MAIL ADDRESS:

Dept. of Physics - Indiana University
Bloomington, IN 47405
Office: 812/855-9421 Fax: 812/855-0440
dzierba@ind.physics.indiana.edu

C. IS THIS PROPOSAL BASED ON A PREVIOUSLY SUBMITTED LETTER OF INTENT ?

[x] YES [ ] NO

IF YES, TITLE OF PREVIOUSLY SUBMITTED LETTER OF INTENT:

A Measurement of Rare Radiative Decays of the ϕ Meson

(CEBAF USE ONLY)

Receipt Date 4/14/96

Log Number Assigned PR 94-016

By L. Smith

Coordinates of Institutional Contact People

Hall Crannell
The Catholic University of America
Office: 202/319-5313 Fax: 202/319-4448
crannell@cua.edu

Elton Smith
CEBAF
Office: 804/249-7625 Fax: 804/249-5800
elton@cebaf.gov

Scott Teige
Indiana University
Office: 812/855-4623 Fax: 812/855-0440
ind::teige

John LoSecco
University of Notre Dame
Office: 219/631-6044 Fax: 219/631-5952
losecco@nd.edu

Jim Napolitano
Rennselaer Polytechnic Institute
Office: 518/276-8019 Fax: 518/276-6680
jimnap@rpimep.phys.rpi.edu

Billy Bonner
Rice University
Office: 713/527-4897 Fax:
bonnerphysics.rice.edu

Phil Rubin
University of Richmond
Office: 804/289-8254 Fax: 804/289-8482
rubin@urvax.urich.edu

Dinko Pocanic
University of Virginia
Office: 804/924-7691 Fax: 804/924-4576
pocanic@virginia.edu

David Armstrong
College of William and Mary
Office: 804/221-3489 Fax: 804/221-3540
armd@physics.wm.edu

Proposal
to the Continuous Electron Beam Accelerator Facility

Measurement of Rare Radiative Decays of the ϕ Meson

H. Crannell, J. O Brien and D. Sober
The Catholic University of America, Washington, DC 20064

V. Burkert, M. Kossov, B. Niczyporuk and E. Smith
Continuous Beam Accelerator Facility, Newport News, VA 23606

B. Brabson, R. Crittenden, A. Dzierba, J. Gunter, R. Lindenbusch, D. Rust, P. Smith, E. Scott, T. Sulanke and S. Teige
Indiana University, Bloomington, IN 47405

J. Bishop, N. Cason, J. Kolata, J. LoSecco, A. Sanjari and W. Shephard
University of Notre Dame, Notre Dame, IN 46556

G. Adams, J. Napolitano and M. Witkowski
Rensselaer Polytechnic Institute, Troy, NY 12180

B. Bonner, G. Mutchler and S. Ahmad
Bonner Nuclear Physics Lab at Rice University, Houston, TX 77251

G. Gilfoyle, P. Rubin and M. Vineyard
University of Richmond, Richmond, VA 23173

E. Frlez and D. Pocanic
University of Virginia, Charlottesville, VA 22901

D. Armstrong
College of William and Mary, Williamsburg, VA 23187

Spokesperson: Alex Dzierba
Indiana University

Co-Spokesperson: Jim Napolitano
Rensselaer Polytechnic Institute

Abstract

The ϕ meson provides a laboratory for probing the nature of scalar and pseudoscalar mesons. These studies can be accomplished by analyzing the decays $\phi \to f_0(975)\gamma \to \pi^0\pi^0\gamma$, $\phi \to a_0(980)\gamma \to \pi^0\eta\gamma$ and $\phi \to \eta'\gamma$. The branching ratios of these as yet unobserved modes are expected to be of order 10^{-4} to 10^{-5}. Indeed, experiments are planned to study these decays in e^+e^- collisions at *DAΦNE* and *VEPP2M*. Experiments which study ϕ's in flight, such as in photoproduction, have a distinct advantage over those which study ϕ's produced at rest. The problems, in the latter, of detecting and measuring the very-low-energy radiated photon in association with states whose masses are close to that of the ϕ are much less severe when the ϕ, and therefore the radiated photon, are boosted. We propose to install a lead glass calorimeter in the tagged photon beam in Hall B to study decays of the ϕ into all-photon final states to measure these radiative decays. In a 30-day run, with a 4 GeV photon beam of intensity 5×10^7 / *sec* we expect to achieve a branching ratio sensitivity of about 10^{-5} .

0. Organization

1. Physics Motivation

a. Introduction - The Richness of Vector Meson Physics

The vector mesons provide a splendid laboratory for the study of fundamental physics. Witness the factories being contemplated, planned or under construction to collide electrons and positrons at *cms* energies near or at the mass of the ϕ *(ϕ - factory)*, the J/ψ *(τ/charm - factory)* and the Y *(B - factory)*. These projects are justified by the wealth of physics already uncovered by studying the decays of these vector mesons. Trying to understand the decays of the ϕ led to the OZI rule. Decays of the J/ψ and Y and their radial excitations have already provided important information about light-quark and heavy-quark spectroscopy and tests of the standard model. Prominent among the decays are the radiative decays of these states. Photoproduction of the ρ, ω, ϕ, *and* J/ψ has also provided insight into the quark structure of matter and the nature of the coupling of the photon ($J^{PC} = 1^{--}$) to vectors ($J^{PC} = 1^{--}$). The suppression and/or enhancement of the ϕ and J/ψ are being suggested as possible signatures for the onset of the quark-gluon plasma in relativistic heavy-ion collisions.

b. Radiative Decays of the ϕ

There is still physics to be uncovered in the study of radiative decays of the ϕ. It is interesting that although there are a number of mesons which are energetically accessible through the radiative decay of the ϕ, only *two* radiative modes have been observed. The decay $\phi \to \eta\gamma$ occurs with a branching ratio of 1.3 % and $\phi \to \pi^0\gamma$ has a branching ratio about a factor of 10 smaller. This already is an interesting result which points to the $s\bar{s}$ content of the η.

The paucity of other observed modes is due in some cases to conservation principles; for example the decays $\phi \to \rho\gamma$ and $\phi \to \omega\gamma$ are C-violating. For decays which are otherwise allowed, the kinematics of the decay, to a large extent, explains why some decays have not yet been observed. Before discussing explicit decays of the ϕ, a review of the decay kinematics is in order. Consider the decay $\phi \to X\gamma$ in the rest frame of the ϕ. The energy of the photon, E_γ, is given by

$$E_\gamma = \frac{m_\phi^2 - m_X^2}{2m_\phi}$$

If $m_X \sim m_\phi$ then $E_\gamma \sim m_\phi - m_X$. As we will see below, many of the interesting decays correspond to masses, m_X, which are of order 1 GeV. In these cases, the radiated photon has just several tens of MeV of energy, which makes experimental detection difficult. A way to circumvent this problem is to produce boosted ϕ's. For example, in the photoproduction process $\gamma p \to \phi p$, the ϕ is produced in the very forward direction with essentially the beam momentum. The boost factor for the radiated photon can be as high as $2 \cdot E_{beam}/m_\phi$. For a tagged photon beam at initial CEBAF energies, this factor is as high as 8.

The small values of E_γ also damp rates for $\phi \to scalar + \gamma$ and $\phi \to pseudoscalar + \gamma$ since these proceed through electric and magnetic dipole transitions respectively and involve E_γ^3 in the final rate, apart from any matrix element contributions. To appreciate the effect of this strong dependence on E_γ, consider the expected ratio of the branching ratios of $\phi \to \eta'\gamma$ relative to $\phi \to \eta\gamma$ ignoring any

difference in the quark or gluon content of the final state mesons:

$$\frac{BR(\phi \to \eta' \gamma)}{BR(\phi \to \eta \gamma)} = \left[\frac{m_\phi^2 - m_{\eta'}^2}{m_\phi^2 - m_\eta^2} \right]^3 = 4 \times 10^{-3}$$

We will now consider a number of ϕ radiative decay modes.

c. $\phi \to a_o \gamma$ *and* $\phi \to f_o \gamma$

These are decays of the ϕ into a scalar meson state and a photon and therefore their rates suffer from the E_γ^3 dampening. The first of these scalar states is an isovector and the second is an isoscalar. They are nearly degenerate in mass. For completeness their properties are:

a_o: $I^G = 1^-$ $J^{PC} = 0^{++}$ $m = 980$ *MeV* $\Gamma = 57$ *MeV*
f_o: $I^G = 0^+$ $J^{PC} = 0^{++}$ $m = 975$ *MeV* $\Gamma = 47$ *MeV*

The isoscalar state decays into $\pi\pi$ while the isovector state decays into $\eta\pi$. Both states also decay into KK. The question of the interpretation of these states as $q\bar{q}$ states is an intriguing one and has attracted much theoretical attention [1]. For example the masses and widths are inconsistent for a P-wave $q\bar{q}$ nonet. The proximity of these states to the $K\bar{K}$ threshold complicates the picture. Moreover the ${}^3P_o$ $q\bar{q}$ nonet is oversubscribed adding to the real possibility that these may be *non* $-$ $q\bar{q}$ states, for example $qq\bar{q}\bar{q}$ or $K\bar{K}$ molecules.

The authors of ref [2] show how a measurement of the ratio of branching ratios of ϕ radiative decays can provide information on the makeup of these scalar states. In the conventional ${}^3P_o$ $q\bar{q}$ picture we expect $(\phi \to a_o\gamma)/(\phi \to f_o\gamma) = 0$ because of OZI suppression. The $K\bar{K}$ *molecule vs* $qq\bar{q}\bar{q}$ pictures can be distinguished by the electric dipole nature of these decays (which probes the electric charges of the constituents weighted by the distance from the overall *cm*) through the relative phases in $I = 0$ and $I = 1$ wavefunctions and through the relative spatial distributions of quarks and antiquarks. To summarize:

${}^3P_o$ $q\bar{q}$ *nonet:*

$$\left.\begin{array}{l} a_o = (u\bar{u} - d\bar{d})/\sqrt{2} \\ f_o = some\ s\bar{s} \end{array}\right\} \Rightarrow \frac{\phi \to a_o\gamma}{\phi \to f_o\gamma} = 0$$

$K\bar{K}$ *molecule:*

$$\left.\begin{array}{l} a_o \\ f_o \end{array}\right\} = \frac{1}{\sqrt{2}}\left[(u\bar{s})(\bar{u}s) \mp (d\bar{s})(\bar{d}s) \right] \Rightarrow \frac{\phi \to a_o\gamma}{\phi \to f_o\gamma} = 1$$

$qq\bar{q}\bar{q}$:

$$\left.\begin{array}{l} a_o \\ f_o \end{array}\right\} = \frac{1}{\sqrt{2}}\left[(us)(\bar{u}\bar{s}) \pm (ds)(\bar{d}\bar{s}) \right] \Rightarrow \frac{\phi \to a_o\gamma}{\phi \to f_o\gamma} = 9$$

d. $\phi \to$ *scalar* $+ \gamma$ *and implications for CP studies at a* $\phi -$ *factory*

The measurements of the branching ratios discussed above is important information for CP studies at a $\phi -$ *factory*. The decay sequence $\phi \to K^o\bar{K}^o \to K_L^o K_S^o$ occurs because the spin of the ϕ requires the anti-symmetric $K_L^o K_s^o$. This means that CP-studies can be performed at a $\phi -$ *factory* by tagging the K_s^o which thereby tags the K_L^o. However, the presence of the radiative decay

$$\phi \to (K_S^o K_S^o \ \ or \ \ K_L^o K_L^o)\gamma$$

will complicate or possibly destroy CP studies at a e^+e^- $\phi -$ *factory* if the branching ratio is higher than 10^{-4} since at a $\phi -$ *factory* [3] the radiated photon, which has at most $m_\phi - 2 \cdot m_K = 30$ *MeV* of energy, will escape detection. The measurement of the radiative decays into scalars will provide information on this potentially insidious background to CP studies. At the current measured limits (which do not provide the guarantee that CP physics can be done at a $\phi -$ *factory*), we will observe a few tens of thousands of decays into scalar states. Ref [2] includes a discussion of how the explicit rate for $\phi \to K_s^o K_s^o \gamma$ can by extracted from a measurement of $\phi \to \pi^o\pi^o\gamma$ and $\phi \to \eta\pi^o\gamma$.

e. $\phi \rightarrow \eta' \gamma$

This decay mode is strongly damped because of the mass of the η' relative to the ϕ. The measurement of this branching ratio is important in providing information on the gluonic and $s\bar{s}$ content of the η' [4,5].

f. $\phi \rightarrow \eta\gamma$ *and* $\phi \rightarrow \pi^o\gamma$

These modes have already been observed and are well measured. Although the proposed experiment will not contribute new information about these modes, a measurement of these decays and their ratio will be an important monitor in this proposed experiment. As we show in Section 4, we expect to see about 150,000 $\phi \rightarrow \eta\gamma$ decays.

g. $\phi \rightarrow \rho\gamma$ *and* $\phi \rightarrow \omega\gamma$

These modes are C-violating but the current limits on them are very imprecise and of order several percent. The sensitivity of the proposed experiment is such that the limit on $\phi \rightarrow \omega\gamma$ should be improved by 3 to 4 orders of magnitude.

h. Other physics

i) $\phi \rightarrow \omega\pi^o$ is an isospin violating decay which has not been observed. From the measured branching ratio of $\phi \rightarrow \rho\pi^o$ we expect the branching ratio for the isospin violating decay to be of order 10^{-4}. We will search for this mode in this proposed experiment.

ii) Radiative decays of the ρ *and* ω. In a photoproduction experiment, we expect a rich sample of ρ *and* ω. This experiment provides an opportunity to improve the measurement of the branching ratios of $\rho \rightarrow \pi^o\gamma$ and $\omega \rightarrow \eta\gamma$. The isospin-violating decay $\omega \rightarrow \eta\pi^o$ has not been observed.

iii) Production and observation of the C(1480). The C(1480) has been observed by only one group [1] as a $\phi\pi^o$ resonance with a likely J^{PC} assignment of 1^{--}. Its OZI-violating branching ratio of $\phi\pi : \omega\pi$ makes it unlikely that it is a $q\bar{q}$ state [1]. It has been pointed out [6] that a photoproduction experiment is ideally suited for studying such a state. Under the assumption of vector-dominance and pion exchange, if the C(1480) is a diquark-diquark state with hidden strangeness, the expected cross section for $\gamma p \rightarrow Cp \rightarrow \phi\pi^o p$ at 4 GeV is about *0.1* μb.

References:

[1] See the discussion of these states and other candidates in the Review of Particle Properties (1992).

[2] F. Close, N. Isgur and S. Kumano, Nucl. Phys. B389 (1993) 513

[3] G. Barbiellini *et al,* Particle World, 1 (1990) 138.

[4] F. Lenz, Nucl. Phys B279 (1987) 119. This paper also discusses the structure of the f_o.

[5] J. L. Rosner, Phys Rev D27 (1983) 1101.

[6] B. Kopeliovich and E. Predazzi preprint IUHET-271 and private communication with the authors.

2. Experimental Setup and Implementation

a. Introduction

The proposal is to install a 25×25 element lead glass detector (LGD) in the Hall B tagged photon beam in front of the CLAS detector. A similar detector is shown in fig 2.1 and the placement in Hall B is shown in fig 2.2. The proposal assumes 5×10^7 *tagged 4 GeV photons/sec*. The beam will be incident on a 1-in thick Be target which will be followed by a charged particle veto (CPV) downstream of the target. The CPV will be used to veto on the presence of charged particles in the final state. The array will be large enough to match the transverse dimensions of the lead glass array but will not intercept recoil protons from the ϕ production reaction: $\gamma p \rightarrow \phi p$. The kinematics of the recoil proton is shown in the distribution of fig 2.3

It may be that the optimal place for the charged particle veto is just upstream of the LGD. This is

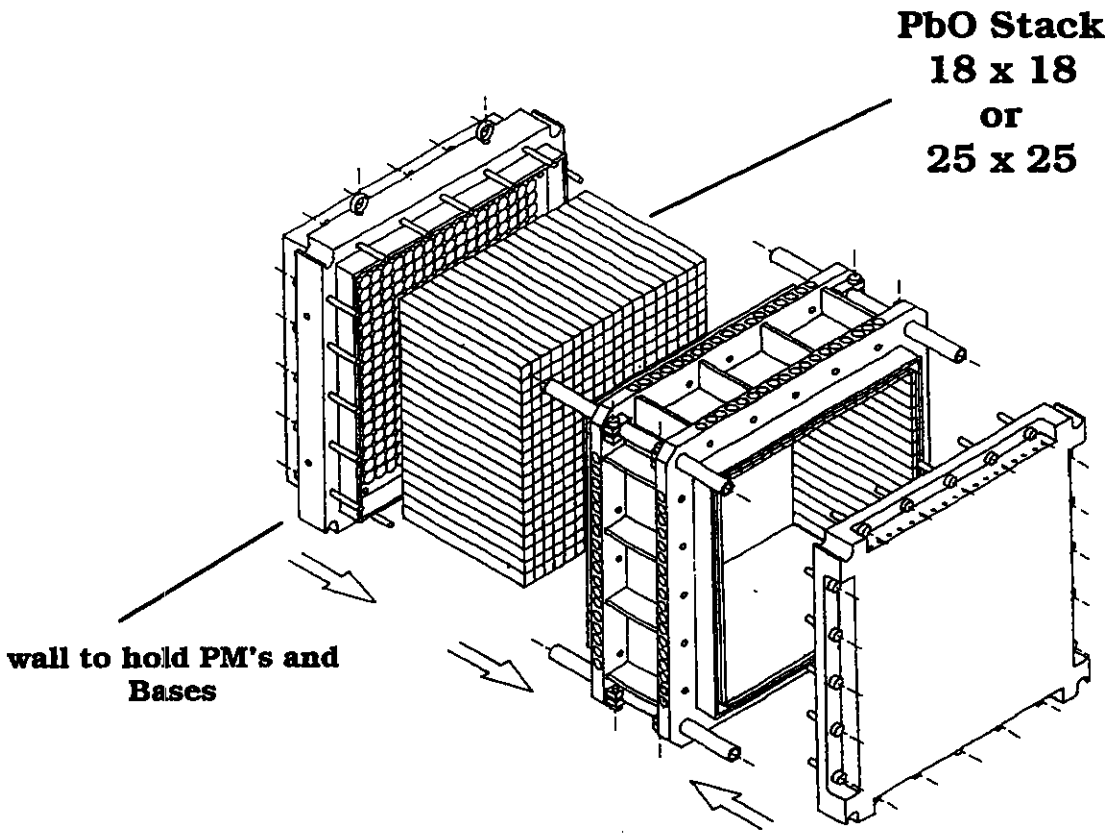

Fig 2.1: Schematic of the lead glass detector

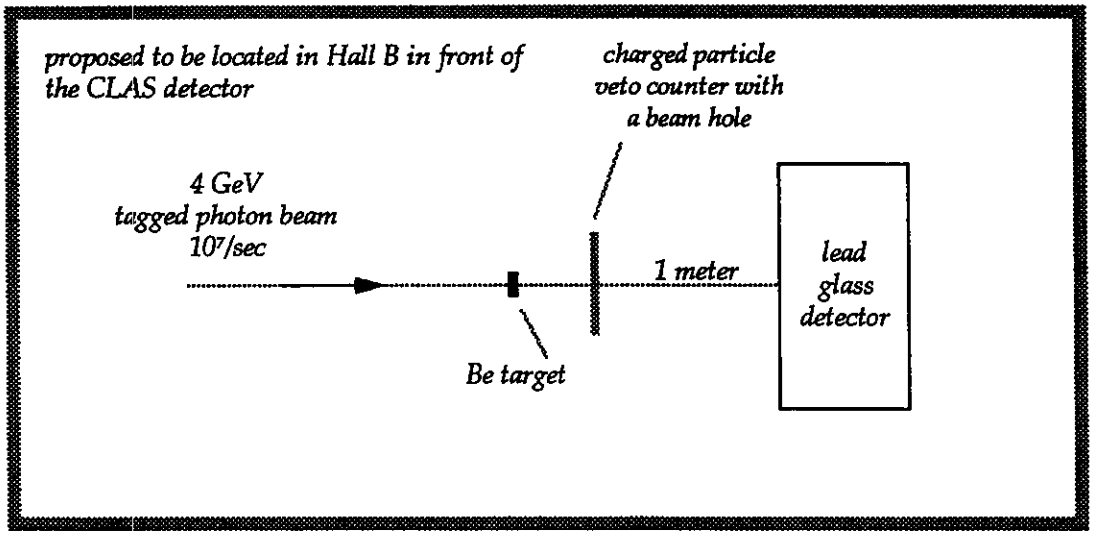

Fig 2.2: Proposed installation of the detector in Hall B

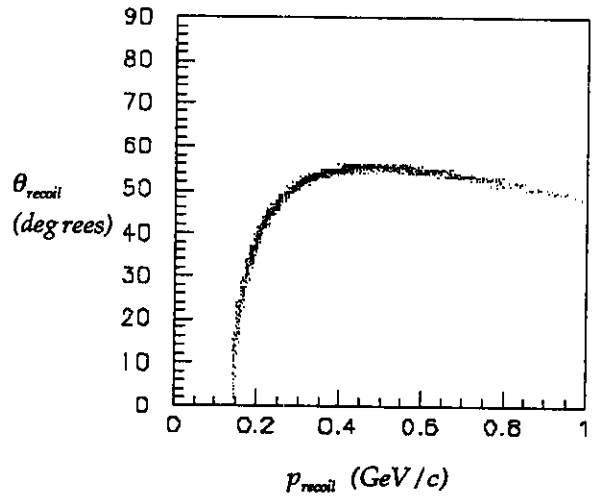

Fig 2.3: Direction (angle with respect to beam) and momentum of the recoil proton in ϕ photoproduction at 4 GeV.

being studied. The lead glass detector and the CPV will have holes for passage of the non-interacting photon beam. A 4-cm diameter vacuum pipe will be used between the target and the LGD to minimize material presented to the non-interacting photon beam between the target and LGD.

b. Lead Glass Calorimeter

The lead glass stack is very similar to the array described in ref [1] of the Appendix which summarizes the performance of an array used in a test run at Brookhaven in 1992. The glass blocks are *4 cm by 4 cm* in transverse dimensions and *41 cm* long. The glass has a radiation length of *3 cm* and an interaction length of *22 cm*. Russian phototubes are used and a computer-controlled high voltage system employing Cockcroft-Walton bases is employed. A plexiglass sheet, situated at the front face of the glass, is used to distribute light from a laser to each of the blocks. The monitoring system is used during the run to look for gain changes and at setup time to check out cabling and overall system performance.

The monitoring system, glass, phototubes and bases are enclosed in a light-tight box which sits atop a computer-controlled transporter. The transporter is used to position each block of the array in an electron or photon beam for calibration purposes. The box is also air-conditioned. The weight of the detector including transporter is approximately *3 tons*.

The energy resolution of the detector can be parameterized as

$$\frac{\sigma}{E(GeV)} = \left[2 + \frac{5}{\sqrt{E(GeV)}}\right]\%$$

Energy sharing is used to determine photon positions with $\sigma_{x,y} = 5\ mm$.

c. Data Acquisition and Triggering

The standard CEBAF data acquisition system, CODA, together with the slow controls system will be used to acquire data and control the experiment. A Level 1 trigger will be obtained by either discriminating an analog signal of the summed output of the LGD or using an array of wavelength shifter strips along back of the lead glass stack (between the phototubes) to integrate light. The total hadronic production rate is about *150 KHz*, the tagged rate between 2 and 4 GeV is *18 KHz*, for a tagged photon rate of $5 \cdot 10^7\ \gamma's/sec$.

The signals from the detector are digitized by a custom-built ADC system which has 32 channels per FASTBUS module. The 12-bit ADC s can present their results to a trigger processor in $4\ \mu sec$. A noise-subtraction technique insures good noise immunity and there are also two levels of discriminated output well before the 12-bit digital output. The reset time of the ADC is *200 ns*.

A trigger processor finds photon clusters and computes energies and positions (or equivalently the photon 3-vectors). The processor can be used to form a trigger based on these results (e.g. total energy, number of photons, total effective mass, di-photon effective masses). The trigger processor can be invoked at a rate of 18 KHz for a dead time of less than a few percent.

d. Implementation and Responsibilities

Table 2.1 summarizes the institutional responsibilities for the construction of this experiment. This division of responsibilities is tentative and of course subject to funding at the various institutions.

Institution	*Responsibilities*
Catholic U.	Photon tagger
CEBAF	Data acquisition system, 1st level trigger
Indiana U.	Lead glass, phototubes, bases, ADC's, transporter, trigger electronics
U. of Notre Dame	Charged particle veto, splitters and summers for the fast prterigger and vacuum pipe
Rensselaer Polytechnic Institute	Photon tagger
Rice U.	Photon tagger, online software
U. of Richmond	Online software and data acquisition, cables
U. of Virginia	Monitoring system for calorimeter
College of William and Mary	Trigger electronics

Table 2.1: Tentative Institutional Responsibilities

3. Acceptance Estimates

a. A First-Order Estimate of Geometric Efficiencies

In order to optimize the experimental geometry and to estimate the general features of the acceptance for various decay modes of the ϕ we generated Monte Carlo events of the reaction $\gamma p \rightarrow \phi p$ at an incident beam momentum of *4 GeV*. The experimentally observed momentum transfer distribution from incoming beam to outgoing ϕ of eq (3.1) was used. For the decays $\phi \rightarrow (spin\ 0)\gamma$, the decay angular distribution of eq (3.2) was used in the rest frame of the ϕ.

$$\frac{d\sigma}{dt} = const \cdot e^{-1.8|t|} \qquad (3.1)$$

$$\frac{dN}{d\cos\theta} = const \cdot (1 + \cos^2\theta) \qquad (3.2)$$

The schematic of fig 3.1 shows the front face of a 25×25 lead glass array. We assume the central block is removed for passage of the beam. All the other blocks are instrumented. We define the fiducial volume as shown in fig 3.1. An event is accepted if all photons from a decay enter the fiducial volume. Our experience with a prototype lead glass calorimeter (see the reference given in the Appendix) gives us confidence that photons which strike the detector at least *6 cm* from the center of the detector can be reconstructed. We require the minimum separation between any two photons in the fiducial volume be *6 cm*. Finally we considered two minimum photon energy requirements : *150 MeV* and *250 MeV*. In analyzing data from a prototype calorimeter, we have determined that π° reconstruction is possible with a minimum photon energy requirement of *100 MeV*.

In fig. 3.2 we consider the decay $\phi \rightarrow a_o(980)\gamma \rightarrow \eta\pi^\circ\gamma \rightarrow 5\gamma$. The distribution in energy of the highest and lowest energy photon in the event is shown in figs 3.2 (a) and (b). In fig 3.2 (c) the distribution in angle, with respect to the beam direction, of the lowest energy photon is shown. In fig 3.3 (d) a scatter plot of angle *vs* energy of the radiative photon is shown. Only accepted events are plotted and the minimum energy requirement was *150 MeV*.

In fig 3.3 we show the variation of acceptance (in percent) with the target to detector distance. Four decays are considered: $\phi \to \pi^o\gamma \to 3\gamma$, $\phi \to \eta\gamma \to 3\gamma$, $\phi \to f_o(975)\gamma \to \pi^o\pi^o\gamma \to 5\gamma$ and $\phi \to a_o(980)\gamma \to \eta\pi^o\gamma \to 5\gamma$. The acceptance for the first two decays is quite good. It will be important to use these well-determined decays and their observed ratio as a monitor of this experiment. In fig 3.4 we compare the acceptance for the decays $\phi \to f_o(975)\gamma \to \pi^o\pi^o\gamma \to 5\gamma$ and $\phi \to a_o(980)\gamma \to \eta\pi^o\gamma \to 5\gamma$ for two different values of the minimum energy requirement.

In fig 3.5 we show the acceptance for $\phi \to a_o(980)\gamma \to \eta\pi^o\gamma \to 5\gamma$ as a function of the total photon energy folding in the Bethe-Heitler distribution for bremsstrahlung photons from a 4 GeV electron beam. We assume that the production cross-section for the ϕ is independent of energy in this regime. We assume a target-to-detector distance of *100 cm* and the same requirements used for the acceptance curves in fig 3.3. Acceptances for ϕ decays are summarized in Table 5.1. (of Section 5).

b. Understanding the Reconstruction of ϕ Decays with a Hybrid Monte Carlo

In order to estimate reconstruction efficiencies with the proposed experimental layout, a hybrid Monte Carlo simulation was performed. The four-vectors of the decay products from the all-photon decays of the ρ, ω and ϕ (see Table 3.1) were generated as described above with a target-to-detector distance of *100 cm* and data using a similar prototype lead-glass detector (P2 - see the Appendix) were used to simulate the response of the detector proposed for this experiment.

Well reconstructed $\pi^- p \to \pi^o\pi^o n$ events with an incident *15 GeV/c* π^- beam were selected from the P2 data sample. Events were required to have no photons near the hole and a total deposited energy greater than *10 GeV*. The photon momenta were determined using the π^o mass as a constraint. Photon showers were selected from these events. It was required that a selected photon be more than *15 cm* from its nearest neighbor. The energies deposited in the blocks of the reconstructed cluster were written to a file for later use. These showers were indexed by energy (in $\pm$ *300 MeV* bins) and by the reconstructed photon impact point within the central block. (in *1 cm* $\times$ *1 cm* bins).

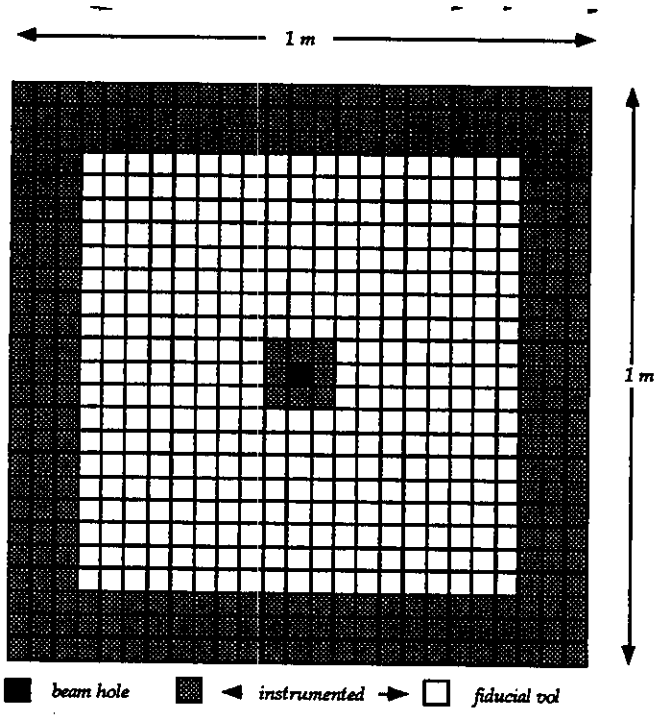

Fig 3.1: A schematic of the front face of a 25 x 25 element lead glass stack. All modules are assumed to be instrumented. The unshaded blocks define the fiducial volume for photon reconstruction.

Each of the blocks has transverse dimensions of 4 cm x 4 cm.

In order for an event to be accepted, all photons have to lie in the fiducial volume, the minimum separation between any two photons is 6 cm and each photon has to exceed E_{min} which can be either 150 MeV or 250 MeV.

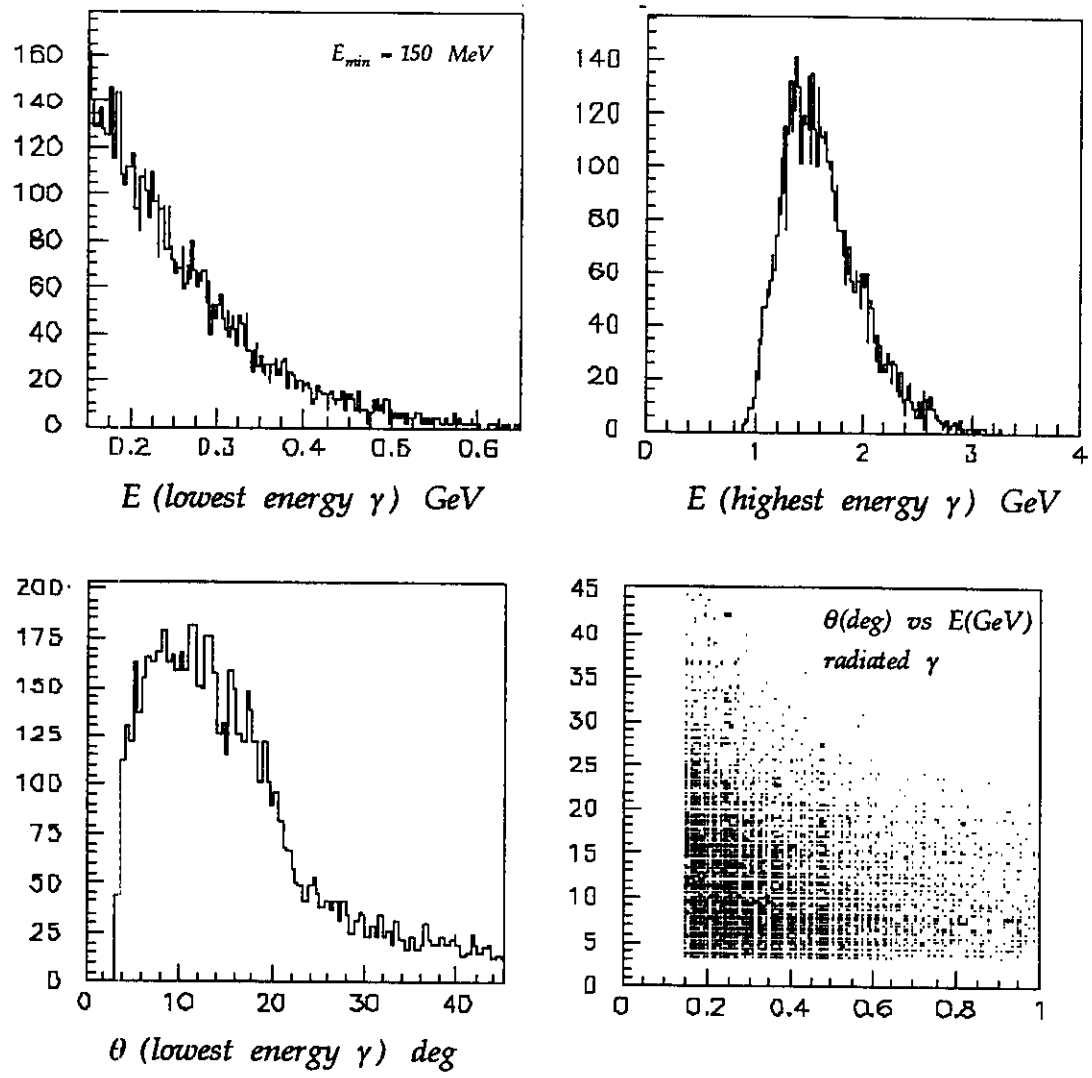

Fig 3.2: Distribution of the (a) energy of the photon with lowest energy; (b) energy of the photon with the highest energy; and (c) angle of the lowest energy photon for the decay $\phi \rightarrow a_0\gamma \rightarrow \eta\pi^0\gamma \rightarrow 5\gamma$. *The scatterplot of the angle vs energy of the radiative photon is shown in (d). Only accepted events are plotted.*

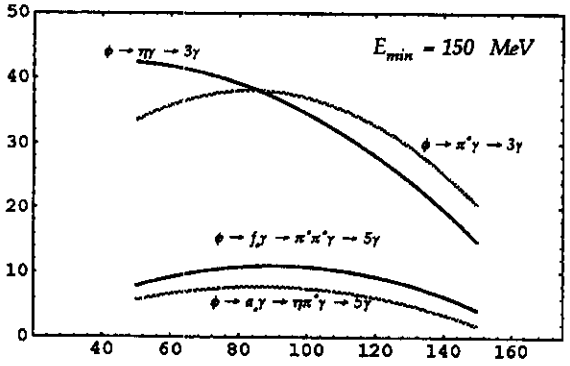

Fig 3.3: Dependence of the acceptance (%) for various ϕ *decays as a function of target to calorimeter distance in cm. The minimum photon energy is 150 MeV.*

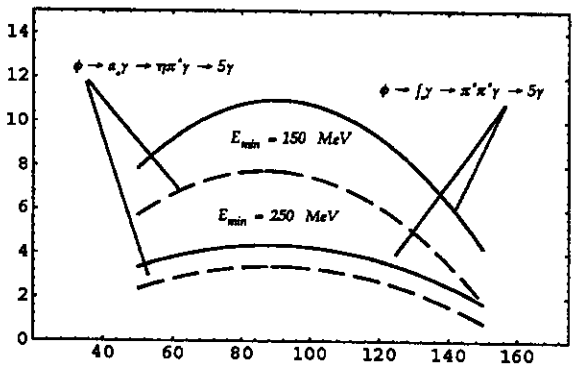

Fig 3.4: Dependence of the acceptance (%) for various ϕ *decays as a function of target to calorimeter distance in cm. Acceptances for minimum photon energies of 150 MeV and 250 MeV are compared.*

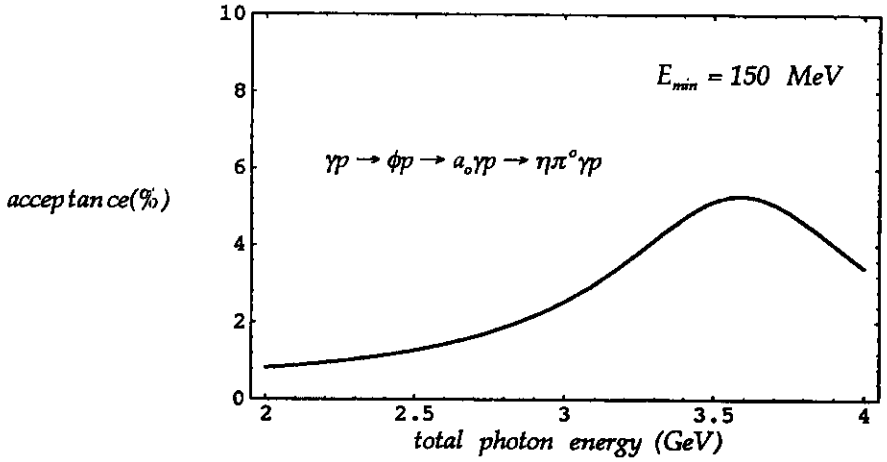

Fig 3.5: Acceptance for the $\phi \rightarrow a_o\gamma$ mode folding in the bremsstrahlung spectrum for the tagged photons with 4 GeV electrons

Decay Mode	Branching Ratio	σ/σ_ϕ
$\phi \rightarrow \eta\gamma$	0.013×0.389 $(\phi \rightarrow \eta\gamma) \times (\eta \rightarrow \gamma\gamma)$	1
$\phi \rightarrow \pi^o\gamma$	0.0013 $(\phi \rightarrow \pi^o\gamma)$	1
$\phi \rightarrow a_o\gamma$	$10^{-4} \times 1/2 \times 0.389$ $(\phi \rightarrow a_o\gamma) \times (a_o \rightarrow \eta\pi^o) \times (\eta \rightarrow \gamma\gamma)$	1
$\phi \rightarrow f_o\gamma$	$10^{-4} \times 1/2$ $(\phi \rightarrow f_o\gamma) \times (f_o \rightarrow \pi^o\pi^o)$	1
$\phi \rightarrow \eta'\gamma$	$10^{-4} \times 0.02$ $(\phi \rightarrow \eta'\gamma) \times (\eta' \rightarrow \gamma\gamma)$	1
$\phi \rightarrow \omega\pi^o$	$10^{-4} \times 0.08$ $(\phi \rightarrow \omega\pi^o) \times (\omega \rightarrow \pi^o\gamma)$	1
$\phi \rightarrow K_S K_L$	0.3391×0.3139 $(\phi \rightarrow K_S K_L) \times (K_S \rightarrow \pi^o\pi^o)$	1
$\omega \rightarrow \pi^o\gamma$	0.08 $(\omega \rightarrow \pi^o\gamma)$	4
$\omega \rightarrow \eta\gamma$	$4 \cdot 10^{-4} \times 0.389$ $(\omega \rightarrow \eta\gamma) \times (\eta \rightarrow \gamma\gamma)$	4
$\rho \rightarrow \pi^o\gamma$	$7.9 \cdot 10^{-4}$ $(\rho \rightarrow \pi^o\gamma)$	36
$\rho \rightarrow \eta\gamma$	$3.8 \cdot 10^{-4} \times 0.389$ $(\rho \rightarrow \eta\gamma) \times (\eta \rightarrow \gamma\gamma)$	36
✓ All unknown branching ratios were taken to be 10^{-4} ✓ We assume 1/2 for the unknown branching ratios: $a_o \rightarrow \eta\pi^o$; $f_o \rightarrow \pi^o\pi^o$		

Table 3.1 Mix of decay modes used for the Monte Carlo study of acceptance and pattern recognition

The photons were tracked to the detector and the struck block was determined. The coordinate of the photon impact in this block was determined. These coordinates, along with the generated energy, determined the index in the file of showers. A shower was read from this file and the block energies were scaled by a factor ($E_{generated} / E_{fitted}$), maintaining the fluctuations in total shower energy. These block energies were added to a 25×25 array simulating the detector so as to simulate any shower overlaps. Energy corresponding to the hole or an area outside the detector was discarded.

Photons with an energy less than *1 GeV* were treated as a special case. It was found from the P2 data that these low energy showers had a significant probability of consisting of a single block. The probability that a shower be a single block (as a function of energy) was determined from the P2 data. The requested (Monte-Carlo) energy was used to determine this probability and a random number generated to determine if a single block shower should be generated. If a single block shower was required a special file was read to give the energy deposition in this single block. Everywhere above *1 GeV*, the probability of a single block shower is less than 1%.

Once the list of energy depositions was determined, the photon clusters were reconstructed using a cluster finding algorithms developed for the experiment described in the Appendix. The algorithm proceeds as follows:

1) Scan the list of blocks for the largest depositied energy.
2) Tag this block and its 8 nearest neighbors as belonging to this shower.
3) Iterate until no untagged block with an energy greater than *350 MeV can* be found.
4) Associate all untagged blocks with showers if they are within the second generation of blocks around the central block. Tag these blocks.
5) Search for untagged, isolated blocks with an energy greater than *100 MeV*.
6) Associate any neighboring blocks with these showers.

The method has been extensively tested with P2 data. The algorithm was constructed as it was to first find higher energy, isolated showers and then find very low energy showers. This choice of algorithm is a compromise between two competing effects: Loss of low energy showers due to too high an energy cutoff in the first level search and creation of artificial showers due to too low an energy cutoff. This compromise was *tuned* for the P2 data and will have to be *retuned* for the proposed experiment.

Once the showers have been found, the photon impact positions are calculated using a linear energy weighting method to find the center of gravity. The photon momentum vector can be constructed using the photon energy and position information and assuming that the photon originated in the target. For these studies, a vertex in the center of a 1x1x1 cm target is assumed. The photon 4-vectors are determined and passed to the *hypothesis sorter*.

Several methods for hypothesis sorting have been investigated. For low multiplicity events (less than about 4) the sorter simply defines a window about the π^o and η mass. If a $\gamma\gamma$ pair is found with an effective mass in this window, the pair is tagged as having the appropriate parent. For higher multiplicity events (greater than about 4) a χ^2 method is used to evaluate the probability of a hypothesis. If parents can be found, the photon energies are fitted using the parent masses as constraints. The parents 4-vectors are calculated and the effective masses of combinations of massive particles and photons are evaluated. Cuts are applied to these masses to select candidates for specific decay modes. This hypothesis-sorting is being refined for the P2 data run and has not been tuned for the proposed experiment

The hybrid Monte-Carlo has been used to estimate the acceptance and reconstruction efficiency for the final states of interest. An event is defined to be accepted if the number of reconstructed showers is exactly equal to the number of generated photons. It is further required that no more than 100 MeV be deposited in the 8 blocks surrounding the hole and that no more than 100 MeV be deposited in the outer two layers of blocks around the detector edges. Table 3.2 gives these calculated acceptances. The comparison of items in Tables 5.1 and 3.2 give some idea of the effect of cluster-finding on acceptance since it is only included in the latter. It is interesting to note that the acceptances for the particular decays of interest ($\phi \rightarrow f_o(975)\gamma \rightarrow \pi^o\pi^o\gamma \rightarrow 5\gamma$ and $\phi \rightarrow a_o(980)\gamma \rightarrow \eta\pi^o\gamma \rightarrow 5\gamma$) are quite similar in the two studies even though the software and LGD response was optimized for a 15 GeV π beam, not for the CEBAF energies of this proposal.

Reconstruction efficiency is more difficult to estimate since it depends strongly the behavior of the hypothesis sorter but by requiring that the number of reconstructed clusters equals the number of generated photons assumptions on the minimum achiev-

Decay Mode	Acceptance (%)
$\phi \to \eta\gamma$	8
$\phi \to \pi^\circ\gamma$	11
$\phi \to a_\circ\gamma$	3
$\phi \to f_\circ\gamma$	5
$\phi \to \eta'\gamma$	14
$\phi \to \omega\pi^\circ$	2
$\omega \to \pi^\circ\gamma$	17
$\omega \to \eta\gamma$	23
$\rho \to \pi^\circ\gamma$	32
$\rho \to \eta\gamma$	28

Table 3.2: Acceptances (in %) based on finding the right number of photon clusters. The photon finding algorithm was optimized for the experiment described in the Appendix.

able photon separation are removed. The requirement of minimal energy deposition in hole and edge blocks removes the artificial assumptions about the size of the fiducial area of the detector. Based on our studies so far, the reconstruction efficiency for $\phi \to f_\circ(975)\gamma \to \pi^\circ\pi^\circ\gamma \to 5\gamma$ is better than 50 %.

The $\pi^\circ\gamma$ effective mass from $\omega \to \pi^\circ\gamma$ events is shown in fig 3. 6. A Gaussian fit yields a mass and σ of *0.78 GeV* and *59 MeV* respectively. The $\eta\gamma$ effective mass from $\phi \to \eta\gamma$ events is shown in fig 3. 7. A Gaussian fit yields a mass and σ of *1.02 GeV* and *56 MeV* respectively. The $\pi^\circ\pi^\circ$ effective mass for reconstructed events simulating $\phi \to f_\circ(975)\gamma \to \pi^\circ\pi^\circ\gamma \to 5\gamma$ is shown in fig 3.8. The $f_\circ \to \pi^\circ\pi^\circ$ is clearly seen.

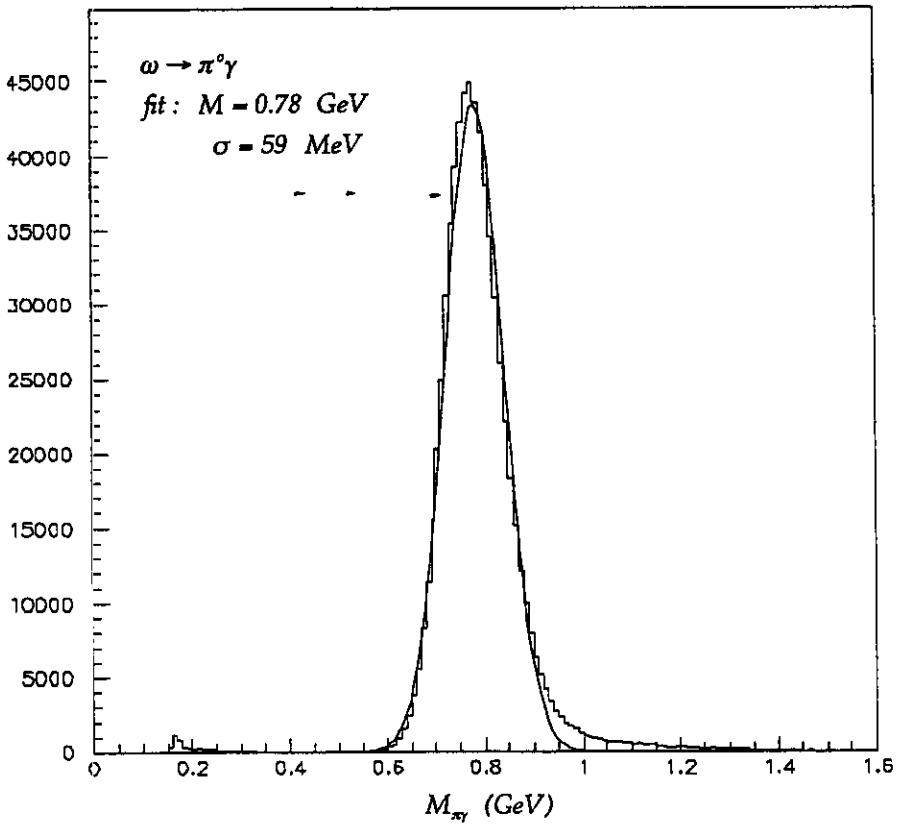

Fig 3.6: Reconstructed ω mass

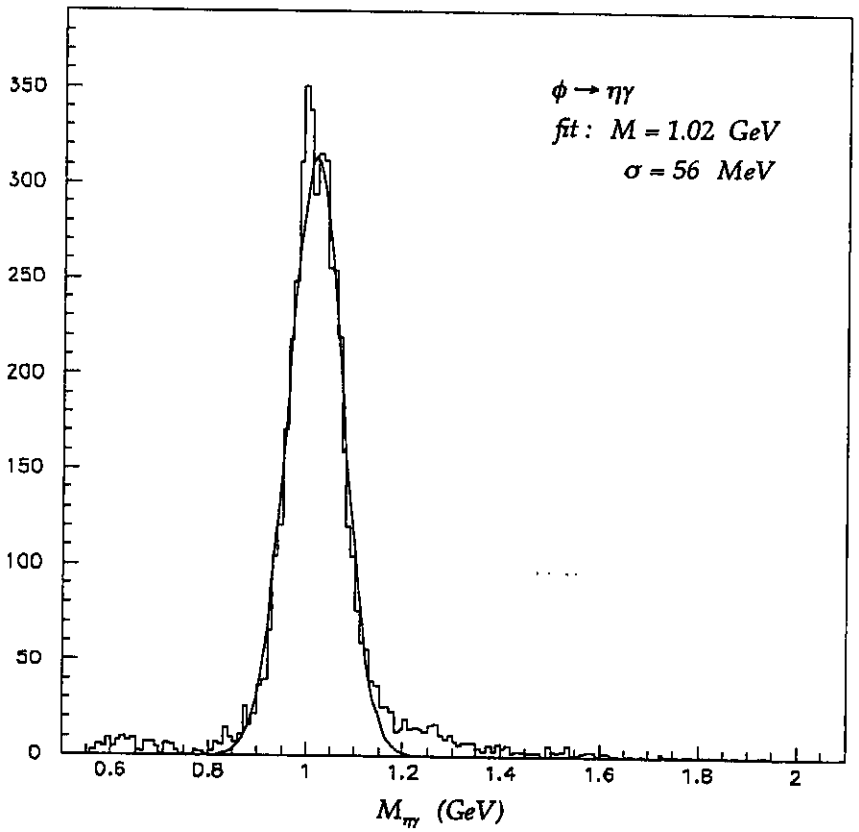

Fig 3.7: Reconstructed ϕ mass

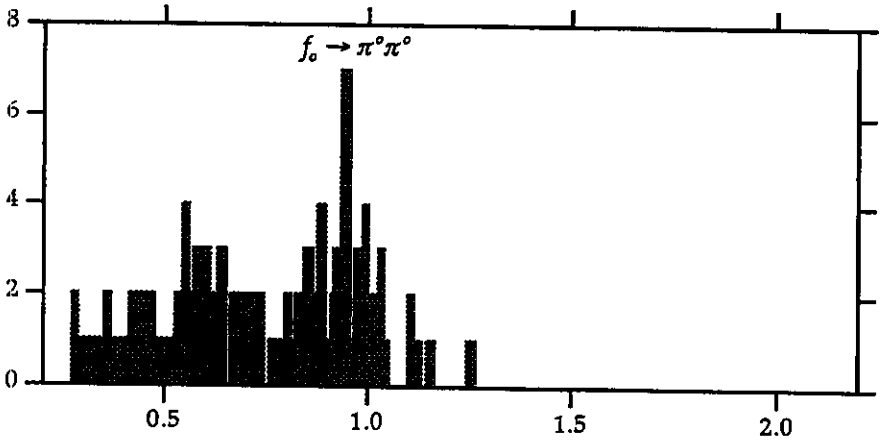

Fig 3.8: The $\pi^o\pi^o$ effective mass for reconstructed events from $\phi \rightarrow f_o\gamma \rightarrow \pi^o\pi^o\gamma$

c. Prospects for the Proposed Experiment

The above shows that even without any retuning of the software used for the P2 test run, we can expect to reconstruct showers and full events to yield reasonable acceptances and widths after event reconstruction. We expect improvements over the estimates from the hybrid Monte Carlo studies since there is an inherent quantization of shower positions in the method which leads to degrading of mass resolutions. We expect other improvements due to the following:

1. the phototube and ADC gains will be optimized for lower energies (i.e. the proposed experiment at 4 *GeV* rather that the P2 test at 15 *GeV*)

2. optimization of a calibration for the appropriate energies and based especially on the high-rate radiative process: $\omega \rightarrow \pi^{o}\gamma$.

4. Backgrounds

d. Hadronic Backgrounds

Hadronic backgrounds are not expected to pose a problem since the estimated rate into the detector should be tens of KHz at most.

The events of interest consist of multi-photon decays of the ϕ and ω. Most of the trigger rate corresponding to all-neutral, multi-photon final states with a total energy exceeding some threshold will be due to $\gamma p \rightarrow \pi^{o} p$. The total rate for this process produced by photons above *1 GeV* is *6.5 KHz*. The trigger processor will have to be invoked to remove these events by employing a total effective mass requirement.

e. Electromagnetic Background

The electromagnetic backgrounds for this experiment come from at least two sources. A 2 *cm* Be target presents about *6%* of a radiation length so about *6%* of the incident beam can be expected to interact. The major process at high energy is pair production. All pairs are produced at small angles and would exit the downstream end of the target inside of the downstream vacuum pipe. The produced pairs have a 6% chance on average of re-scattering in the target. This gives rise to a *0.4%* background. In general only one of the particles in the pair will scatter and so the event would be below trigger threshold. This background scales as the square of the target thickness so the signal to noise could be optimized at the expense of a loss in event rate. The presence of re-scattered pairs makes it essential that the vacuum pipe be extended downstream of the target to at least the end of the detector (as described in Section 2).

The second source of background comes from the large number of photons with energies well below those of interest for ϕ production. Photons with energies below the tagger threshold are still present in the beam and pass through the target. While they will never produce triggerable energy depositions they do contribute to the radiation exposure of the detector and the general noise.

GEANT was used to simulate electromagnetic processes with an incident photon spectrum given by the Bethe-Heitler formula. A tagged photon rate between 2 GeV and 4 GeV of $5 \cdot 10^{7}$ / *sec* was assumed, which means a total photon rate for photons from *10 MeV* to *4 GeV* of $6 \cdot 10^{8}$ / *sec* The energy deposited per area per second as a function of radius from the center of the LGD is shown in fig 4.1. The width of the ADC gate is *250 ns*.

The results are that for blocks at *6 cm* radius (i.e. the innermost layer) we expect an average of *2.4 MeV* per block per ADC gate, from beam-induced background. The average *hit* energy that produces this is *10-15 MeV*. Thus the average of *2.4 MeV* means (Poisson-distributed) that many blocks have nothing, but about 20 % have a 10-15 MeV photon. Since a real shower is spread over several blocks, one must add up over (typically) 9 blocks to get the photon energy. Thus there is a pedestal to the ADC signals of order *25 MeV*. This is negligible compared to the resolution of the lead-glass. The same calculation at *20 cm* radius (near the middle of the detector) gives an order-of-magnitude lower average energy, i.e. completely negligible.

There will, however, be some high-energy showers (due to photons and electron-positron pairs) produced by the beam. Using the same assumptions as above, *4%* of the time there will be a hit somewhere in the detector above *150 MeV*, and *0.1%* of the time a hit above *250 MeV*. This is potentially serious, on first glance, however a large fraction will be cut by the charged-veto. It may be necessary to use TDC information from the lead glass, since these photons will be uncorrelated in time with the real events, and the ADC gate is wide compared to the inherent time resolution of the detector.

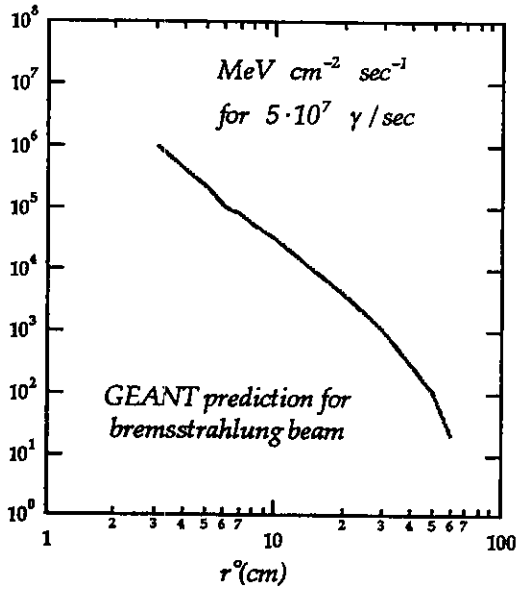

Fig 4.1: Flux of energy at the LGD face as a function of distance from center

5. Yields and Conclusions

The expected yields in a 30 day run are shown in Table 5.1 along with the assumptions made. These yields indicate that the goals of this experiment are readily achieved. Comparable levels of sensitivity will not be achieved until the DAΦNE *φ–factory* is built at Frascati and the KLOE detector is in operation which might happen in mid-1996. The sensitivity of our proposed experiment exceeds by a factor of 10 the sensitivity of 10^{-4} which could be achieved by the experiment operating at VEPP2M. The data are collected but not yet analyzed. There are plans to install a neutral detector in VEPP2M sometime in the future [1]. The proposed experiment at CEBAF represents a real opportunity to make an important contribution to this physics. It is competitive in time and will be done with very different systematics, avoiding the delicacy of the low-energy photons at a stationary ϕ factory.

[1] Private communication with Prof. Julia Thompson (University of Pittsburgh)

Table of Expected Yields

Assumptions: 1-in Be target, σ_ϕ = *0.5 μb* for *4 GeV* photons at 5×10^7 *tagged photons/sec*
Yield: *2.5 million φ's/day* *For acceptance estimates the minimum photon energy is 150 MeV*

Decay Mode $\phi \rightarrow$	*BR(%)*	*BR in all photons* 10^{-4}	*Number of photons*	*Acceptance (%)*	*Acceptance times BR* 10^{-4}	*Yield of Events in 30 Days*
$\pi^\circ\gamma$	0.13	13	3	35	4.5	38,000
$\eta\gamma$	1.3	52	3	35	18.2	150,000
$\eta'\gamma$ ✓	0.04	0.09	3	30	0.03	250
$\omega\gamma$ ✓	5	43	4	20	8.6	75,000
$\omega\pi^\circ$ ✓✓	0.001	0.09	5	10	0.01	75
$a_o\gamma \rightarrow \eta\pi^\circ\gamma$ ✓	0.10	10	5	7	1	5,300
$f_o\gamma \rightarrow \pi^\circ\pi^\circ\gamma$ ✓	0.20	20	5	10	2	15,000

✓ *the measured limit is used* ✓✓ *no limit has been measured, a prediction is used*

For the $\eta'\gamma$ *mode the prediction is about 15 % of the current measured limit*

The following BR are used : $\eta \rightarrow 2\gamma$ *(39 %);* $\eta' \rightarrow 2\gamma$ *(2.2 %);* $\omega \rightarrow \pi^\circ\gamma \rightarrow 3\gamma$ *(8.5 %)*

Table 5.1: *Expected yields for a 4 GeV Tagged Photon Beam*

Appendix: Performance of a Prototype Lead Glass Calorimeter (P2)

Since we propose the use of a lead glass calorimeter to analyze multi-photon final states, we include here a brief description of the performance of a prototype lead glass calorimeter which also was used to collect data on multi-photon final states. This prototype was built and tested by the Indiana University and University of Notre Dame physicists who are also members of the collaboration submitting this letter. In 1992 data were taken with a 18 x 18 lead glass array very similar to the calorimeter being proposed in this letter of intent [1]. This detector was used in a beam of *15 GeV* π^- with a 1-in thick Be target. The target was surrounded in the forward direction with a scintillator veto system to define an all-neutral trigger, i.e., charged beam particle in and no charged particles in the forward direction. Data were collected with target-to-LGD separations of 2 *m* and 4 *m*. At 4 *m*, the photons from the most energetic π^o's are separated by at least 8 cm at the lead glass detector face, allowing for excellent π^o reconstruction. Data were taken with the 2 *m* geometry to challenge the pattern recognition software (this was, after all, a test run) and to increase the acceptance for high mass meson states.

Since it is essential to complete the physics program outlined in this letter in a timely way, it is important to note that the calorimeter was calibrated in less than 12 hours of beam time by moving each module into an electron beam for three complete scans. Within 12 hours of initial data-taking the π^o and η decays into 2γ were observed (see fig (a) on the next page). The data summarized in the plots of the facing page were taken in two weeks of running. Many of the distributions shown were available as the data were collected. The software was able to analyze final states with up to 6 photons in the final state.

Figs (a) and (b) summarize data collected with a 4 *m* target-to-detector distance. The remaining plots summarize data collected at the 2 *m* geometry. Fig (a) shows a plot of the 2γ effective mass distribution for two-cluster events. The π^o and η mass resolutions are *10 MeV* and *21 MeV* respectively. Fig (b) shows the $\pi^o\pi^o$ effective mass distribution for 4-cluster events in which there was a successful constrained fit to $\pi^o\pi^o \to 4\gamma$. The K^o_s is observed in this plot. In this and subsequent plots, the presence of a π^o or η implies a successful constrained fit.

Fig (c) shows a plot of the 2γ effective mass distribution for two-cluster events collected at the 2 *m* geometry. The π^o/η ratio is decreased relative to the distribution shown for the 4 *m* geometry since in some cases the 2γ from π^o's coalesce at the detector face and are not identified as two separate clusters. This coalescence explains the observation of the ω in this plot. In this case, the π^o from the decay $\omega \to \pi^o\gamma$ is detected as a single cluster. Note that the $\eta' \to 2\gamma$ is also observed. In (d) the $\pi^o\gamma$ mass distribution is plotted for three-cluster events. Note the presence of the peaks corresponding to the ω and the $f_2(1275)$. The latter is seen in the $\pi^o\pi^o$ effective mass distribution of fig (e). The reason it is also seen in fig (d) is again due to merging of the 2γ from one of the π^o's. The decays of the $a_o(980)$ and $a_2(1320)$ into $\eta\pi^o$ are observed in the plot of fig (f). Five-cluster events which satisfy constrained fits to $\pi^o\pi^o\gamma$ are summarized in figs (g) and (h). In fig (g) the ω is observed in the $\pi^o\gamma$ effective mass distribution (2 entries/event). In the plot of fig (h) the $\omega\pi^o$ mass distribution is shown for events which contribute to the peak of fig (g) with the constrained fit to $\omega \to \pi^o\gamma$. The $b_1(1235) \to \omega\pi^o$ is observed. In figs (i) and (j), six-cluster events which reconstruct to $\pi^o\pi^o\pi^o$ and $\eta\pi^o\pi^o$ respectively are summarized. The η and η' are observed.

[1] Nucl Instr & Meth, A332 (1993) 419

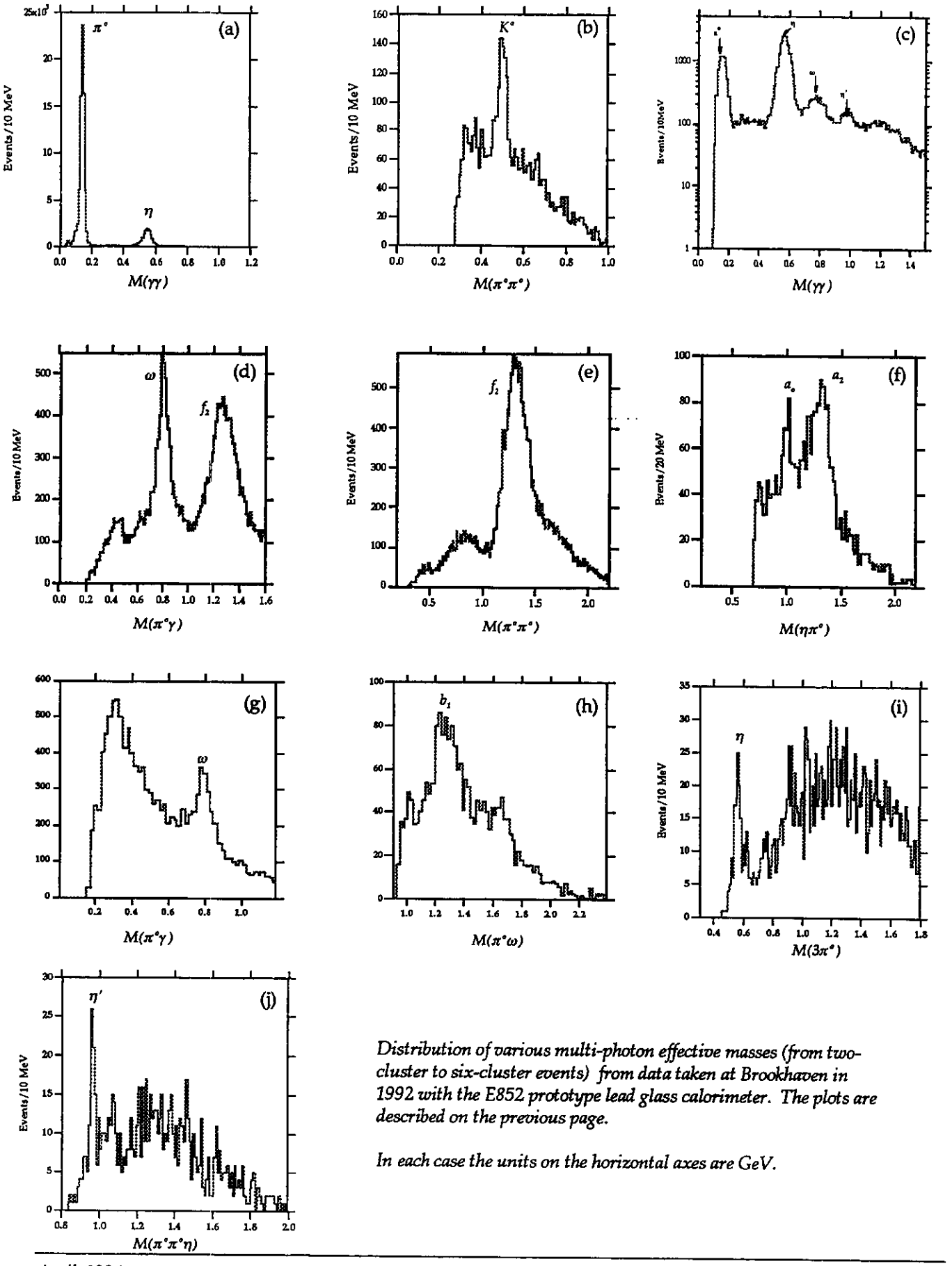

Distribution of various multi-photon effective masses (from two-cluster to six-cluster events) from data taken at Brookhaven in 1992 with the E852 prototype lead glass calorimeter. The plots are described on the previous page.

In each case the units on the horizontal axes are GeV.